Canadian Journal of
Forest Research

Review

Maps depicting the within-tree wood property variation of some North American conifers: a review

Laurence Schimleck[a], **Joseph Dahlen**[b], **Christian Mora**[c], **Finto Antony**[d], **Thomas L. Eberhardt**[e], and **Ighoyivwi Onakpoma**[a]

[a]Department of Wood Science and Engineering, College of Forestry, Oregon State University, Corvallis, OR 97331, USA; [b]Warnell School of Forestry and Natural Resources, University of Georgia, 180 E. Green Street, Athens, GA 30602, USA; [c]Fibraconsult, Concepcion 4030000, Chile; [d] fintoa@gmail.com Hoover, Alabama, USA; [e]USDA Forest Service, Forest Products Laboratory, One Gifford Pinchot Drive, Madison, WI 53726, USA

Corresponding author: **Laurence R. Schimleck** (email: laurence.schimleck@oregonstate.edu)

Abstract

Knowledge of wood property variation within trees is critical for understanding age effects on wood formation and for improved utilization of forests, and maps provide an effective way to efficiently summarize and visually represent variability. Despite the importance of maps, examples for North American conifers are rare. Most studies focus on plantation grown trees, with the majority examining loblolly and radiata pine. For these species almost all maps can be categorized into two groups related to tracheid differentiation processes. One group includes properties related to secondary cell wall formation, e.g., density, and the second relates to tracheid enlargement, e.g., tracheid length. Maps for trees from natural forests are largely limited to density and are highly variable indicating site effects are large. The degree of variation within a species made it impossible to develop conclusions regarding general patterns of variation as with plantation grown trees. The identified density maps are consistent with the three radial variation patterns defined by Panshin and de Zeeuw (1980) (Type 1 (increase), 2 (decrease then increase), and 3 (decrease)). A focused research effort to better visualize wood property variation is required, particularly for species demonstrating Type 2 and 3 radial density patterns.

Key words: North American conifers, within-tree variation, wood and fiber quality, wood property maps

Introduction

Knowledge of how wood properties vary within trees is critical in developing an understanding of how a variety of factors including environment, silvicultural treatment, and age, effect wood property variation, and also for the improved utilization of wood as a raw material (Defo et al. 2009; Leitch and Miller 2017). Regardless of the wood property, variation is observed axially (with height) and radially (pith-to-bark) and both have frequently been independently examined for commercially important North American conifers (Okkonen et al. 1972; Panshin and de Zeeuw 1980; Schimleck et al. 2022). However, our understanding of wood property variation within-trees has been constrained by the cost, time, and difficulty of examining the large number of samples required to achieve the level of detail necessary to illustrate radial and axial variation together. Owing to these limitations, many studies of wood property radial variation are limited to samples from breast height only (Schimleck et al. 2022) and research examining axial variation have typically relied on the estimation of density on whole discs collected at multiple heights (Okkonen et al. 1972).

Improvements in wood property measurement techniques now allow relatively rapid measurement of a wide range of wood properties. The emergence of radiation-based densitometry in the 1960s (Phillips 1960; Phillips et al. 1962; Polge 1964; Harris 1969) was a critical development as it allowed the assessment of density at high spatial resolution in large numbers of trees across a variety of species, but more significantly for this review, the development of SilviScan (Evans 1994; Evans 1999; Evans 2006) and calibrated near-infrared (NIR) spectroscopy in the last 30 years now allow information to be collected on multiple wood properties (Schimleck and Tsuchikawa 2021). Properties measured by SilviScan include microfibril angle (MFA), stiffness (as derived from SilviScan measured density and corresponding X-ray diffraction data), and various tracheid parameters (radial and tangential diameter, wall thickness, perimeter, coarseness, and specific surface), whereas NIR spectroscopy allows prediction of properties not measured by SilviScan, e.g., tracheid length (Schimleck and Evans 2004; Via et al. 2005; Nabavi et al. 2018), and those directly related to wood chemistry such as cellulose, extractives, and lignin content, as well as pulp yield

(Schimleck and Tsuchikawa 2021). With the increased sophistication of measurement techniques, wood property data are more readily available than at any point in the past. However, owing to the variety of properties that can be examined concurrently, increases in the spatial resolution of the data radially, and greater sampling intensity (multiple heights per tree and number of trees sampled), it has become increasingly challenging to present the collected data in a succinct way that is easy to interpret and understand.

Wood property maps provide an effective way to efficiently summarize and visually represent variability (Defo et al. 2009; Leitch and Miller 2017) and allow patterns in two-dimensional data to be discerned that would not be apparent when their one-dimensional constituents, i.e., radially and axially, are examined either in isolation or together. These maps are a logical extension of the earliest studies that endeavored to show a two-dimensional representation of density variation for North American conifers. Early studies utilized data measured at relatively low resolution, depicted radial variation at a small number of heights and focused on individual trees. Species examined included longleaf pine (*Pinus palustris* Mill.) (Fernow 1896) (Fig. 1), "virgin-growth" redwood (*Sequioa sempervirens* (D. Don) Endl.) (Luxford and Markwardt 1932) (Fig. 2) and western white pine (*Pinus monticola* Douglas ex D. Don) (Paul 1963), and while they did not produce maps, they should be recognized owing to their attempts to depict within-tree variation. The first maps for North American conifers were published in the early 1960s for red pine (*Pinus resinosa* Sol. ex Aiton) (Cooper 1960) (Fig. 3) and black spruce (*Picea mariana* (Mill.) B.S.P.) (Risi and Zeller 1960) (Fig. 4) but an examination of the literature indicates that prior to the development of SilviScan and NIR spectroscopy, wood property maps were relatively rare. In the last 30 years the number of maps reported has increased significantly, as has the number of properties examined. These maps represent an important resource, and the overall aim of this review is to organize available wood property maps in a logical way, and to examine if, collectively, they can be used to enhance our understanding of wood property variation within trees and amongst species.

Our examination of maps representing within-tree variation of wood properties indicates that two broad groups of maps exist. One group represents work done on plantation grown species (predominately pines) with most maps being for loblolly pine (*Pinus taeda* L.) and radiata pine (*Pinus radiata* D. Don). In the first section of the review, we examine maps based on densitometry data (e.g., Evans et al. 1995; Tian et al. 1995*a*; Dahlen et al. 2018), properties measured by SilviScan (e.g., Evans et al. 1995), NIR-predicted properties (e.g., So et al. 2002; Mora and Schimleck 2009), handsheet properties (Schimleck et al. 2021*a*), lignin content, pulp yield (Schimleck et al. 2021*b*), and tracheid length (Dahlen et al. 2021*a*). It is important to note that we are responsible for the majority of the reported publications describing loblolly pine within-tree variability, hence we frequently cite papers we have written in this section. A concerted effort was made by the authors/librarians to search databases using key terms for maps/drawings and wood properties fundamental to the field of wood science; citation lists, and visits to library archives

Fig. 1. Radial variation for specific gravity at three heights for a single longleaf pine. Drawing by Joshua Limbaugh (USDA Forest Service, Forest Products Laboratory, Madison WI) based on a figure shown in Fernow, B.E. 1896. Southern pine-mechanical and physical properties. U.S. Department of Agriculture, Division of Forestry, Circular No. 12. 12 pp.

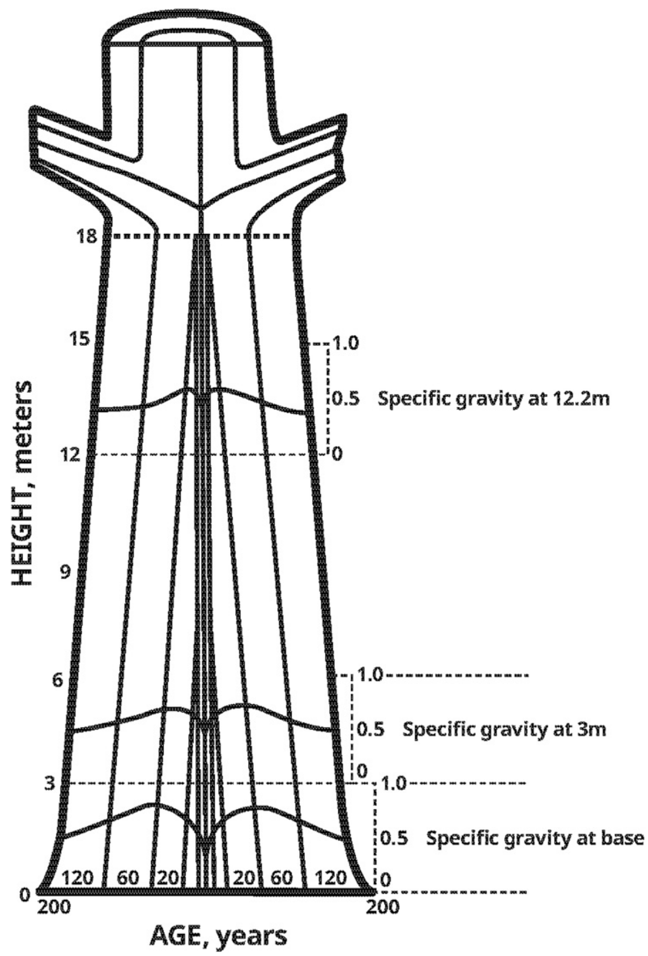

rounded out our effort to provide the most comprehensive review of available wood property maps. The second group represents studies based on a variety of species sampled from natural forests. In most cases only density (or specific gravity (SG) or relative density) was examined and many of the maps were based on single trees. This section of the review is concerned with primarily providing a summary of publications that exist. The final section of the review provides a summary of observations made possible by a collective examination of wood property maps of North American conifers. Future research directions are also proposed.

Wood property maps for plantation grown trees

Table 1 summarizes wood property maps for plantation grown North American conifers and demonstrates the extent to which research has focused on loblolly pine in the southeastern United States, and radiata pine, a species native

Can. J. For. Res. 55: 1–14 (2025) | dx.doi.org/10.1139/cjfr-2024-0142

Fig. 2. Radial variation for specific gravity at six heights for a redwood; solid and dashed lines represent opposite sides of the tree. From Luxford, R.F., and Markwardt, L.J. 1932. The strength and related properties of redwood. Tech. Bull. 305. US Dep. Agric., Washington D.C., 48 p.

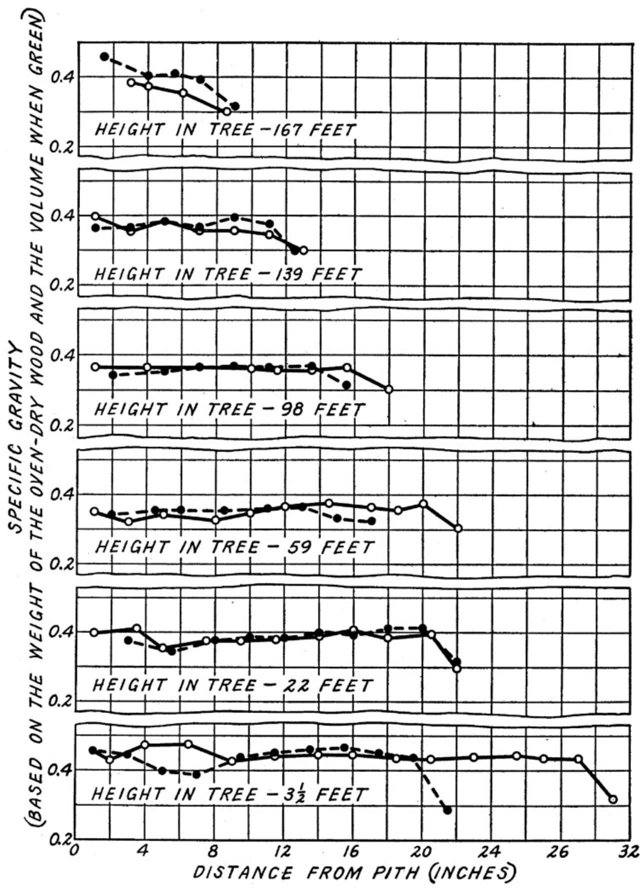

Fig. 3. Example of a specific gravity map for red pine. Drawing by Joshua Limbaugh (USDA Forest Service, Forest Products Laboratory, Madison WI) based on a figure shown in Cooper, G.A. 1960. Specific gravity of red pine as related to stem- and crown-formed wood. Iowa State J. Sci. **34**(4): 337–349.

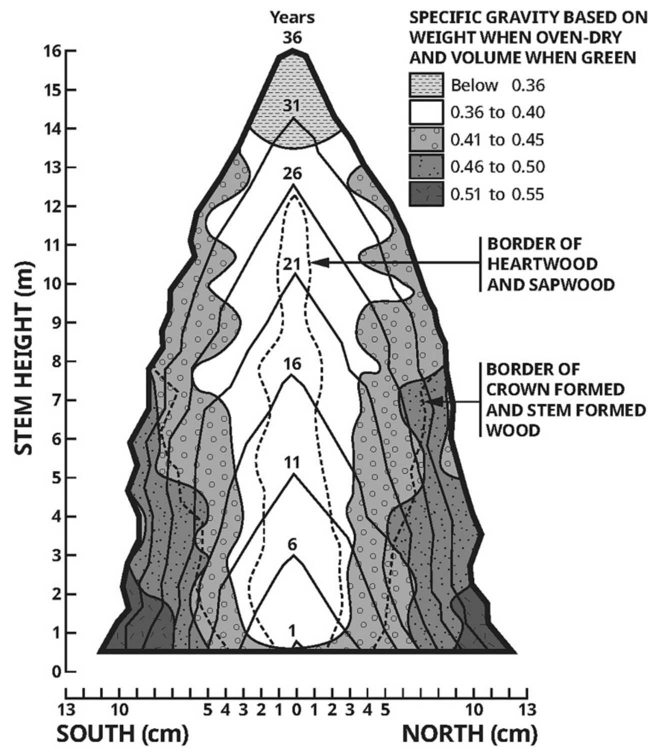

Fig. 4. Example of a specific gravity map for black spruce. From Risi, J., and Zeller, E. 1960. Specific gravity of the wood of black spruce (*Picea mariana* (Mill.) B.S.P.) grown on a Hylocomium-Cornus site type. Laval Univ. For. Res. Found. Quebec, Canada Contr. 6, 70 pp. Reproduced with permission.

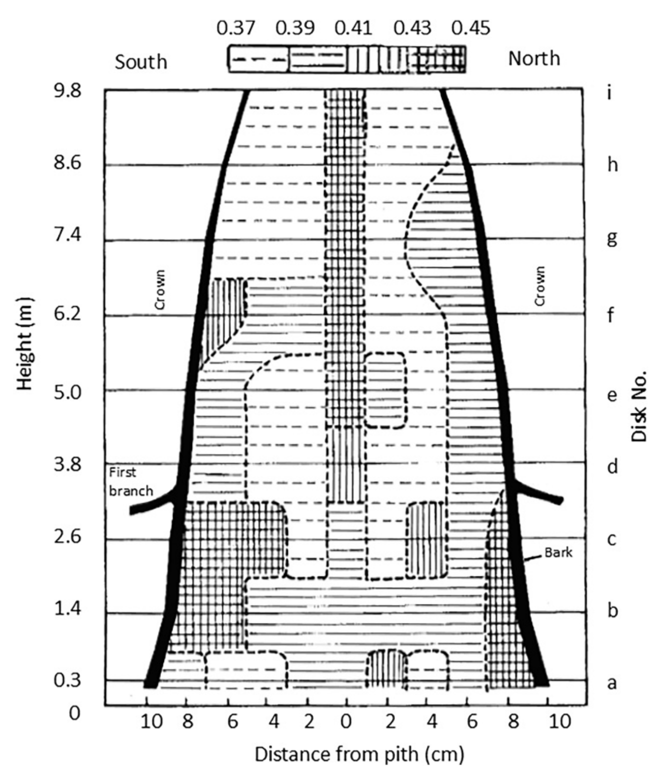

to the coastal regions of central California and Cedros and Guadalupe Islands off the coast of Baha California (Hardin et al. 2001) and an exotic plantation species in the southern hemisphere countries including Australia, Chile and New Zealand. Many maps are based on models developed using measured or NIR-predicted data and publications that utilized models of wood property variation to provide maps (Tian et al. 1995*a*,*b*, Evans et al. 2004; Moore et al. 2014, 2015; Dahlen et al. 2018, 2021*a*,*b*, 2023; Vaughan et al. 2021) are noted. Further, a few maps that appear to be full stem profiles, are actually radial profiles in a single direction that have been replicated (mirror image) to give a full stem profile for aesthetics. Few full stem profiles (wood properties measured and mapped for two cardinal directions (north vs. south, east vs. west), assumed to be opposite each other unless otherwise stated, and at multiple heights) have been published (Cooper 1960; Risi and Zeller 1960; Evans et al. 1995, 2006; Thumm et al. 2016; Eberhardt et al. 2019), and the studies that include two cardinal directions have been identified. Two papers published for plantation grown Douglas-fir (*Pseudotsuga menziesii* (Mirb.) Franco) (Todoroki et al. 2012; Longuetaud et al. 2016) are included in Table 1 but are not discussed further

Table 1. Summary of studies that have mapped within-tree wood property variation for North American conifers from plantations.

Species	Age	Sampling location	Properties mapped	Number of trees per map	Approach used to provide data for mapping	Reference
Douglas-fir	36, 45, 51	Coastal Pacific Northwest	Density, stiffness	1 (20 maps)	Physical testing	Todoroki et al. (2012)
	20, 43	France	Basic SG#	1 (29 maps)	CT scan	Longuetaud et al. (2016)
Loblolly pine	48	Arkansas	Fiber stiffness, fiber ultimate tensile strength, MFA, fiber cross sectional area, fiber quality index	1	Physical testing	Groom et al. (2002); Mott et al. (2002)
	55	Arkansas	SG, stiffness, strength	3	NIR-predicted	So et al. (2002)
	30	Mississippi	Stiffness	3	NIR-predicted	So et al. (2002)
	15	South Carolina	Stiffness	3	NIR-predicted	So et al. (2002)
	22–29	Florida, Alabama and South Carolina	Fiber length, fiber width, fiber wall thickness, basic density, MFA, stiffness, moisture content	1 (3 maps/ property)	SilviScan, gravimetric, maceration	Lundqvist et al. (2005)
	13	Georgia	Density, MFA	6 (3 maps of diff. diam)	NIR-predicted	Mora and Schimleck (2009)
	24–33	Georgia	SG	93	Densitometry*	Dahlen et al. (2018)
	13 and 22	Georgia	Density, MFA, stiffness (at two ages)	18	NIR-predicted	Schimleck et al. (2018)
	13 and 22	Georgia	Coarseness, specific surface, wall thickness, tangential diameter, radial diameter (at two ages)	36	NIR-predicted	Schimleck et al. (2020)
	18–31	Georgia	Tracheid length, tracheid width	268	NIR-predicted*	Dahlen et al. (2021*a*)
	13 and 22	Georgia	Burst index, sheet density, short span compression strength, tensile index (at two ages)	18	NIR-predicted	Schimleck et al. (2021*a*)
	13 and 22	Georgia	Lignin content, pulp yield (at two ages)	18	NIR-Predicted	Schimleck et al. (2021*b*)
	24–33	Georgia	SG, Stiffness (dynamic), ultrasonic velocity	92	Physical testing*	Dahlen et al. (2023)
Longleaf pine	70	Louisiana	SG^{+}, percent $latewood^{+}$, earlywood SG^{+}, latewood SG^{+}	10	Densitometry	Eberhardt et al. (2019)
Radiata pine	N/A	New Zealand	Density (schematic)	N/A	N/A	Cown (1974)
	25 and 50	New Zealand	Alpha cellulose, extractives, lignin (schematic)		Wet chemistry (review paper)	Uprichard and Lloyd (1980)

Can. J. For. Res. 55: 1–14 (2025) | dx.doi.org/10.1139/cjfr-2024-0142

Table 1. (*concluded*).

Species	Age	Sampling location	Properties mapped	Number of trees per map	Approach used to provide data for mapping	Reference
	52	New Zealand	Density, tracheid length (schematic)	10	Gravimetric, maceration	Cown and McConchie (1980); Cown et al. (1991)
	19	Tallaganda, Australia	Density, fiber coarseness[+], fiber perimeter, fiber wall thickness	1	SilviScan	Evans et al. (1995)
	23 and 43	New Zealand	Density	40	Densitometry[*]	Tian et al. (1995*a*)
	22, 26, and 28	Kaingaroa Forest New Zealand	Spiral grain angle	30	Scribed angle measurement[*]	Tian et al. (1995*b*)
	13	New Zealand	Tracheid perimeter, tracheid wall thickness	25	SilviScan	Evans et al. (1999)
	16	New Zealand	Handsheet density	11	Physical testing[*]	Evans et al. (2004)
	38 (approx.)	Western Victoria	Density[+], longitudinal shrinkage[+], MFA[+], spiral grain[+], stiffness[+]	1 (15 butt log maps)	SilviScan	Evans et al. (2006)
	18–33	New Zealand	MFA	347	SilviScan[*]	Moore et al. (2014)
	11–35	New Zealand	Spiral grain angle	1535	Scribed angle measurement[*]	Moore et al. (2015)
	7	New Zealand	Galactan[+]	20	NIR-Predicted	Thumm et al. (2016)
Red pine	36	Iowa	SG[+]	4	Physical testing	Cooper (1960)
Slash pine	30	Mississippi	Stiffness	3	NIR-predicted	So et al. (2002)

Note: A planted forest is defined as "forests in which trees have been established through planting or seeding by human intervention" (Zhang and Stanturf 2008). MFA = microfibril angle, SG = specific gravity. [#]Basic SG is based on CT data collected on discs when green.
[*]Maps based on models developed using measured or NIR-predicted data.
[+]Maps are full stem profiles.

Can. J. For. Res. **55**: 1–14 (2025) | dx.doi.org/10.1139/cjfr-2024-0142

as maps are of single trees and in the case of those published by Todoroki et al. (2012), they are very low in resolution.

Maps for density/SG and related properties

Maps represented in this group display variation that is marked by a radial trend in wood properties, i.e., an increase or decrease from pith to bark. At the pith, an axial trend is absent or not readily apparent but as cambial age increases, variability with height for a given ring is observed to occur. Density/SG is the most frequently examined property amongst this group and it is observed to increase radially and decrease axially (i.e., for rings of the same age at different heights) for loblolly pine (Lundqvist et al. 2005; Mora and Schimleck 2009; Dahlen et al. 2018; Schimleck et al. 2018; Dahlen et al. 2023), radiata pine (Cown 1974; Cown and McConchie 1980; Cown et al. 1991; Evans et al. 1995; Tian et al. 1995*a*), red pine (Cooper 1960) and slash pine (*Pinus elliottii* Engelm.) (So et al. 2002). An example of a SG map for loblolly pine (Dahlen et al. 2023) is presented in Fig. 5. For 70-year-old longleaf pine (Eberhardt et al. 2019) the same initial trends are observed but SG decreased in the outerwood of these trees (which is also reported in Eberhardt et al. 2018, and consistent with other studies of older longleaf and loblolly pine, e.g., Fernow 1896; Eberhardt and Samuelson 2015). The only exception was a loblolly pine map published by So et al. (2002) which showed higher SG values at the tree base extending from outerwood inward to the corewood. Overall radial density/SG variation for the pine species listed in Table 1 is consistent with Type 1 SG variation (SG increases radially to a plateau) as defined by Panshin and de Zeeuw (1980). The pattern of axial density/SG variation is consistent with that reported by Okkonen et al. (1972) for several pine species from the southern USA.

Depending on the method utilized for density/SG measurement and subsequent mapping, map detail and the representation of trends vary. For example, Tian et al. (1995*a*) and Dahlen et al. (2023) developed logistic models describing radial and axial trends, and the published maps were derived from these models. Notable in both is the decreasing trend of density/SG with height. This trend was not apparent for the corewood of density maps based on NIR-predicted values and mapped using an interpolation approach (Mora and Schimleck 2009; Schimleck et al. 2018). The difference may have resulted because the NIR-predicted data lacks the accuracy of the X-ray densitometry data used by Tian et al. (1995*a*) and Dahlen et al. (2023).

Also notable are attempts to depict density variation for individual loblolly pine trees growing on sites of different quality (high, medium, and low site index) (Lundqvist et al. 2005), for groups of loblolly pine from a single location of similar radii (Mora and Schimleck 2009) and for loblolly pine at two different ages (13 and 22 years) (Schimleck et al. 2018). For the different maps in these studies, the variation observed for density remains consistent with that already described; however, density values do differ, for example, the high-density zone increases from age 13 to 22 years (Schimleck et al. 2018), and the largest trees in Mora and Schimleck (2009) have lower density outerwood.

Fig. 5. Map of specific gravity variation in loblolly pine. From Dahlen, J., Auty, D., and Eberhardt, T.L., Schimleck, L.R., and Pokhrel, N.R. 2023. Models for predicting the within-tree variation of ultrasonic velocity and dynamic modulus of elasticity for plantation loblolly pine. Forestry 96(4): 588–604.

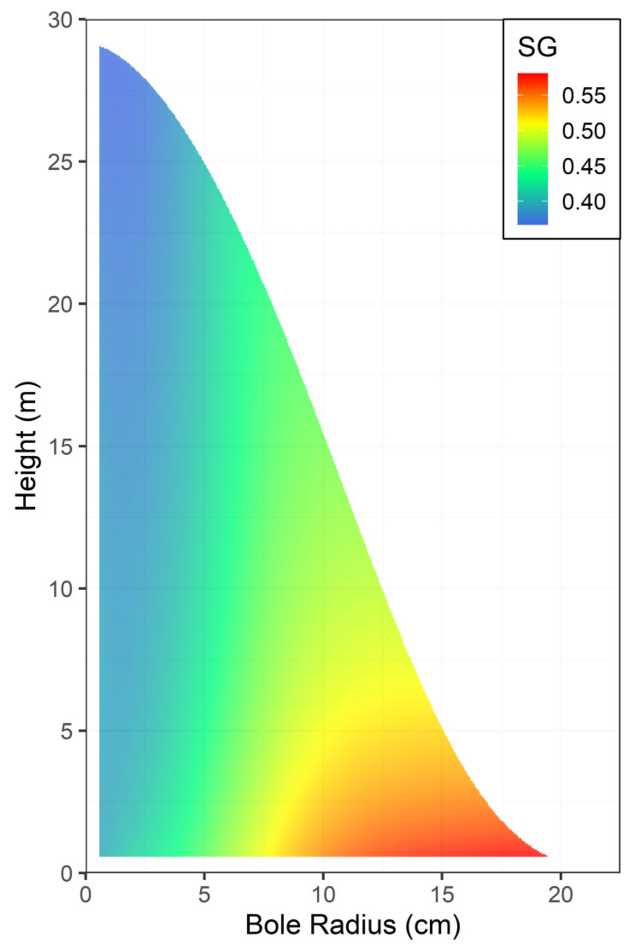

A variety of other properties have been mapped for loblolly, longleaf, and radiata pine (Table 1) and those that have strong positive relationships with density/SG (Evans 1994; Burdon et al. 2004; Li et al. 2014) all have similar maps. Properties include tracheid wall thickness (Evans et al. 1995; Evans et al. 1999; Lundqvist et al. 2005; Schimleck et al. 2020), % latewood and latewood SG (Eberhardt et al. 2019), and tracheid coarseness and specific surface (Evans et al. 1995; Schimleck et al. 2021*a*).

Properties that have negative relationships with density/SG have maps with inverse patterns and include moisture content maps for individual loblolly pine trees from sites of differing quality (Lundqvist et al. 2005), and a lignin content map (Schimleck et al. 2021*b*). A possible explanation for the lignin map is that latewood (which increases radially in loblolly pine) has lower lignin content than earlywood (Downes et al. 2010) which would produce a decrease in ring lignin content as % latewood increases radially. Many handsheet properties are also negatively related to density (Kibblewhite et al. 2003; Evans et al. 2004), and general patterns for their property maps are comparable to density maps

Can. J. For. Res. **55:** 1–14 (2025) | dx.doi.org/10.1139/cjfr-2024-0142

Fig. 6. Map of microfibril angle (MFA) variation in radiata pine. Predicted MFA is based on (*a*) a modified logistic function with a linear relative height term, (*b*) a logarithmic relative height term and (*c*) a modified Michaelis-Menten function with a linear relative height term and (*d*) a logarithmic relative height term. From Moore, J.R., Cown, D.J. and McKinley, R.B. 2014. Modelling microfibril angle variation in New Zealand-grown radiata pine. N. Z. J. For. Sci. 44:25. Reproduced with permission.

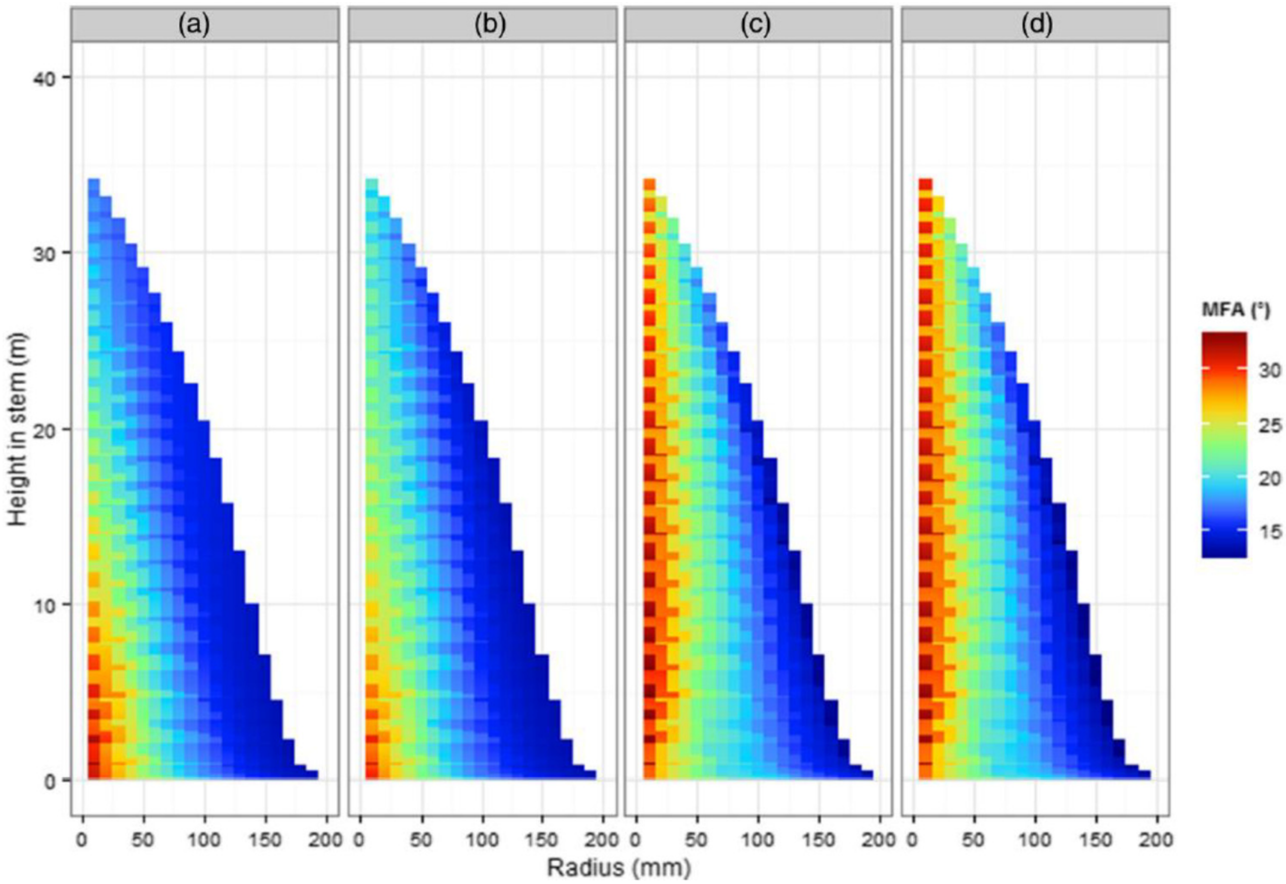

for plantation grown pines though they are the inverse. Examples include predicted handsheet density for an average of 24 radiata pine trees (Evans et al. 2004), and burst index, sheet density, STFI (Swedish Test Fibre Institute) short-span compression strength, and tensile index for loblolly pine (Schimleck et al. 2021*a*). Evans et al. (2004) also reported handsheet density maps for two individual ramets of two different radiata pine clones. Even within a clone there are notable differences between maps for the two ramets, an example of the variability that exists within individuals and a reminder of the importance of considering maps that represent an average of multiple trees, as opposed to single tree maps, when making general conclusions regarding within-tree variability.

Property maps that share similar characteristics to those reported for MFA and stiffness

Additional property maps have been published for loblolly and radiata pine that are visually different from those observed in the previous section for density/SG and related properties and collectively these maps have similar characteristics. Properties in this group of maps increase, e.g., tracheid length (Dahlen et al. 2021*a*) or decrease, e.g., MFA (Lachenbruch et al. 2011) rapidly from pith to bark for the first 5 to 15 years but after this time change slowly. In loblolly pine, it can take 20-plus years for MFA to plateau (Jordan et al. 2007), whereas tracheid length continues to increase but at a rate much slower than observed initially (Dahlen et al. 2021*a*). These maps also show variation in height in the corewood, with most of the axial variability occurring from the stump to a height of 5 m.

MFA variation in radiata pine (Fig. 6) (Moore et al. 2014) provides an example and the variation depicted (which differed slightly depending on the modeling approach utilized by Moore et al. (2014)) is consistent with loblolly pine MFA maps (Lundqvist et al. 2005; Mora and Schimleck 2009; Schimleck et al. 2018). Other properties with similar maps include tracheid length (Cown et al. 1991; Dahlen et al. 2021*a*), stiffness (So et al. 2002; Schimleck et al. 2018), pulp yield (Schimleck et al. 2021*b*), tracheid width (Dahlen et al. 2021*a*), tracheid tangential diameter (Schimleck et al. 2018) and ultrasonic velocity (USV) and dynamic stiffness (Dahlen et al. 2023). Lundqvist et al. (2005) also presented maps for stiffness, tracheid length and width, but owing to the resolution of data for tracheid length or variation across maps for the three individual trees depicted, it is not possible to characterize the maps as similar to those listed earlier in the paragraph.

While the overall patterns are similar, there is some variation between loblolly and radiata pine for maps of MFA. For example, MFA maps for loblolly pine (Mora and Schimleck 2009; Schimleck et al. 2018) show a large region of high MFA for corewood at the tree base, and this zone does not appear as extensive in MFA maps for radiata pine (Moore et al. 2014). Similarly, the zone of low MFA outerwood in radiata pine extends to the base of the tree as MFA radial variation is similar at all examined heights (Moore et al. 2014), whereas in loblolly pine outerwood it does not, as MFA at 1.4 m is consistently higher than other heights (4.6, 7.6, 10.7, and 13.7 m) for an equivalent ring (Jordan et al. 2007). In a recent study Dahlen et al. (2023) mapped USV measured in 10 mm increments on loblolly pine radial strips and a map of velocities showed the highest velocity region (lowest MFA's) extended to the base. Many of the trees examined by Moore et al. (2014) and Dahlen et al. (2023) are older than those examined by Mora and Schimleck (2009) which may explain the observed differences.

Maps for loblolly pine depicting wood stiffness variation (So et al. 2002; Schimleck et al. 2018; Dahlen et al. 2023), display similar variation to MFA maps, particularly in the corewood, likely owing to the strong relationship between MFA and stiffness when MFA is high, e.g., above 25° (Barnett and Jeronimidis 2003). A map for stiffness variation in slash pine (So et al. 2002) is also very similar to those of loblolly pine.

Maps showing pulp yield variation for loblolly pine aged 13 and 22 years reported by Schimleck et al. (2021*b*) are also similar to the corresponding stiffness maps (Schimleck et al. 2018), but a zone of low-yield wood at the center of the tree and up to a height of 3 m is not as large radially as the zone of low stiffness wood. The maps are likely similar as wood high in cellulose can be expected to be both stiff and have a high yield of pulp (compared to wood of lower cellulose content) (Albert et al. 2002; Raymond et al. 2010).

Property maps for plantation grown pines depicting unique characteristics

While most wood properties examined for plantation grown pines can be grouped into two categories (density and MFA/stiffness) there are a small number of studies (Tian et al. 1995*b*; Groom et al. 2002; Mott et al. 2002; Evans et al. 2006; Moore et al. 2015; Thumm et al. 2016) whose property maps are different. The stiffness maps reported by Evans et al. (2006) for 15 radiata pine butt logs are unique owing to their high level of detail in four cardinal directions (Fig. 7). Low stiffness corewood is depicted in all plots with higher stiffness outerwood, however outerwood stiffness values vary considerably amongst and within trees. While the maps are of single logs (not whole-tree), they are important owing to the extent of the variability illustrated when high-resolution data (by ring) is plotted. Another example of a highly detailed and unique map is one showing galactan variation within a radiata pine stem (Thumm et al. 2016). The map was based on hyperspectral images of wood discs which allowed for prediction of wood properties at the pixel level. Zones where galactan increases can be observed but whether this is due to any radial trend or zones of compression wood cannot be ascertained.

Fig. 7. Variation in butt log stiffness in four cardinal directions for fifteen radiata pine trees. Adapted with permission from Evans, R., Ilic, J., Fife, D., Gritton, D., Mattay, J., and Morrow, A. 2006. Comprehensive distribution of wood quality characteristics in pine butt logs. WQI Ltd. Report No. Str 23, 22 p.

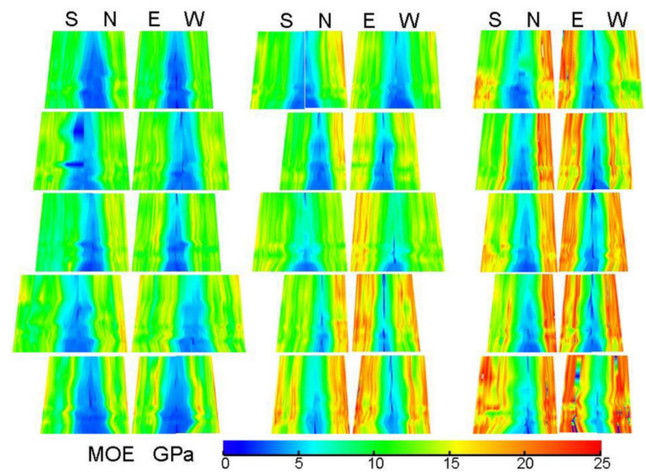

Maps reported by Groom et al. (2002) and Mott et al. (2002) for several properties of a single loblolly pine aged 48 years cannot be compared to other maps owing to the methods used to measure properties, and the depiction of maps with localized variability. Only the map for ring MFA (Groom et al. 2002) appears similar to other MFA maps for loblolly and radiata pine. Maps for spiral grain angle in radiata pine (Tian et al. 1995*b*; Moore et al. 2015) also differ as spiral grain angle decreases linearly from pith to bark with the rate of decline decreasing with increasing height.

Wood property maps for trees from natural forests

Table 2 summarizes wood property maps for North American coniferous species based on trees from natural forests. All listed studies report maps for density/SG with very few reporting maps for additional properties.

Unlike the density/SG maps reported for plantation pines it is not possible to identify any common patterns amongst those listed in Table 2. It is apparent that stand history can have a large impact on within-tree variation and this is illustrated by studies that provide density maps for a single species sampled at different locations, with examples including ponderosa pine (*Pinus ponderosa* Dougl. ex Laws.) (Vaughan 2020), western hemlock (*Tsuga heterophylla* (Raf.) Sarg.) (Jozsa et al. 1998) and coastal and inland varieties of Douglas-fir (Jozsa and Kellogg 1986). For ponderosa pine Vaughan (2020) provided six individual tree maps (three for a site with the lowest median tree-level average density and three for a site with the highest) and all had differing density patterns. Similarly, variation in western hemlock maps (Fig. 8) published by Jozsa et al. (1998), for trees from five locations that differed in age (85–98) and stocking (440 to 1000 trees/ha), make any

Table 2. Summary of studies that have mapped within-tree wood property variation for North American conifers from natural forests.

Species	Age	Sampling location	Properties mapped	Number of trees per map	Approach used to provide data for mapping	Reference
Ponderosa pine	37–170	Arizona	Density	1 (6 maps)	Densitometry*	Vaughan (2020)
Black spruce	70–80	Quebec	SG+	1	Physical testing	Risi and Zeller (1960)
Spruce	140	N/A	Density, MFA, stiffness	1	SilviScan	Downes et al. (2009)
Sitka spruce	<75	Southeast Alaska	SG	217	Densitometry*	Dahlen et al. (2021*b*)
Douglas fir	45, 53, 60	British Columbia (4 locations)	Density	5 (4 maps)	Densitometry	Jozsa and Kellogg (1986)
	30	N/A	Tracheid coarseness	1 (4 maps)	SilviScan	Defo et al. (2009)
Western hemlock	90	British Columbia (5 locations)	Relative density	13 (5 maps)	Densitometry	Jozsa et al. (1998)
	<75	Southeast Alaska	SG	128	Densitometry*	Dahlen et al. (2021*b*)
Western red cedar	85	British Columbia	SG	1	Physical testing	Wellwood and Jurazs (1968)

*Maps based on models developed using measured or NIR-predicted data.
+Maps are full stem profiles. MFA = microfibril angle, SG = specific gravity.

generalizations impossible. However, examination of radial profiles at different heights for the trees examined by Jozsa et al. (1998) indicates radial variation was exclusively Type 2 (SG decreases initially then increases radially to a plateau) as defined by Panshin and de Zeeuw (1980). The Douglas-fir maps reported by Jozsa and Kellogg (1986) were highly variable with trees from one location (Wells Gray) having high-density corewood, that decreased to a low-density plateau in outerwood, whereas maps for Douglas-fir trees from the other locations had high density outerwood. It is important to note that the radial density variation for trees from Wells Gray is one of the few examples of a Type 2 species (Douglas-fir) having a Type 3 (SG decrease radially to a plateau) pattern (Schimleck et al. 2022).

Other common issues with many of maps reported in Table 2 is that often a single tree is examined and its age, when sampled, is quite old relative to the sampling ages of plantation grown trees listed in Table 1. The age of the trees is important as the older the tree the greater the chance it has been exposed to widely different levels of stocking and competition, which represents an extremely different scenario to relatively young trees grown in plantations. The most notable maps in this respect are for density, MFA and stiffness of a single spruce aged 140 years (Downes et al. 2009) that due to the depicted axial-radial variation of properties are very different to those observed for plantation grown trees. Specifically, with extreme values from the pith outward for MFA (lowest end of range) and MOE (highest end of range) at an approximate height of 2 m, with an almost mirror image pattern above and below this height.

Another unique SG map is of an 85-year-old western red cedar (*Thuja plicata* Donn ex D. Don) (Wellwood and Jurazs 1968). A small zone of high SG corewood at the base of the tree is shown, and generally, SG decreases radially, consistent with Type 3 variation. An axial increase in SG is observed above a height of 6 m (total height was 24 m), with the largest region of the densest wood occurring in the upper third of the tree. An axial increase in SG is observed above a height of 6 m (total height was 24 m), with the largest region of the densest wood occurring in the upper third of the tree. On a weighted disc average basis SG has been reported to increase axially in western red cedar (Wellwood and Jurazs 1968; Okkonen et al. 1972).

The only study that reports maps of trees from natural forests that can be considered comparable to some reported in Table 1 is Dahlen et al. (2021*b*) who reported SG maps for Sitka spruce (*Picea sitchensis* (Bong.) Carr.) and western hemlock based on models developed using multi-height (3) samples from 217 and 128 trees, respectively. For both maps a narrow high SG core is present with SG decreasing radially before again increasing in outerwood, i.e., Type 2 as defined by Panshin and de Zeeuw (1980), but they appear quite different (Fig. 9) to each other (and to the density maps listed in Table 1) as there is a trend of increasing SG with height in Sitka spruce (the highest SG corewood is observed in the upper 2/3 of the stem), whereas SG decreases slightly for western hemlock. Interestingly an increasing axial trend is consistent with the map of Risi and Zeller (1960) for black spruce

Fig. 8. Average stem profiles, extent of live crown, and stemwood relative density distribution for western hemlock. From Jozsa, L.A., Munro, B.D., Gordan, J.R. 1998. Basic wood properties of second-growth western hemlock. FPInnovations. (Formerly: Forintek Canada Corp. SP38), 51 p. Reproduced with permission.

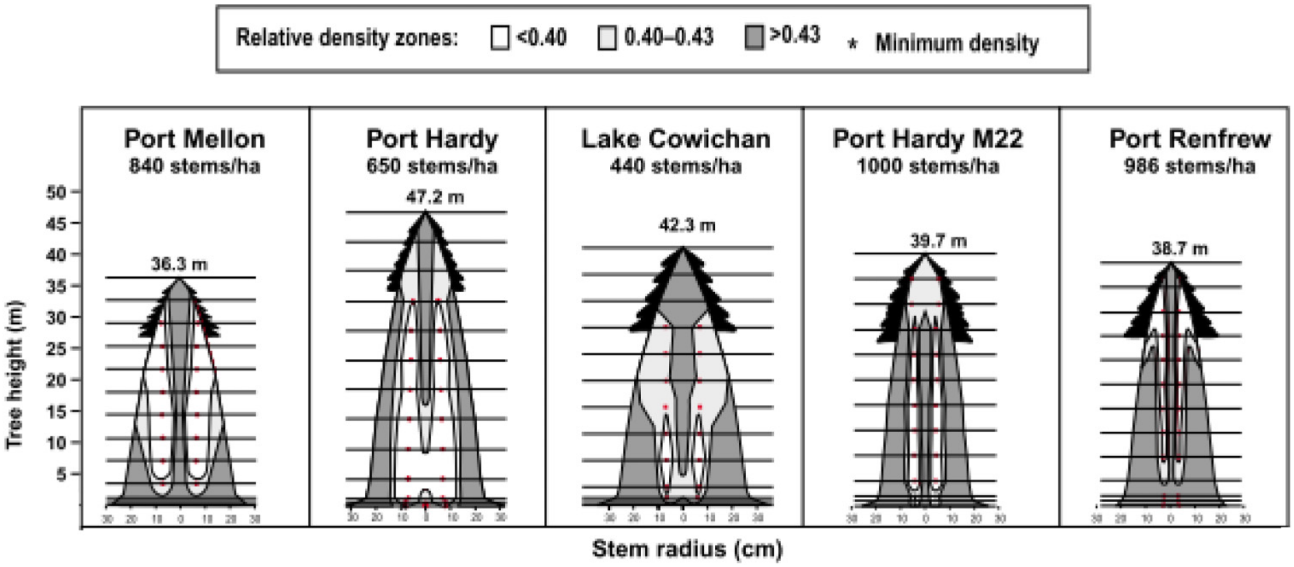

Fig. 9. Maps of specific gravity variation in Sitka spruce and western hemlock. From Dahlen, J., Auty, D., and Lowell, E. 2021b. Modeling specific gravity and diameter inside bark of western hemlock and Sitka spruce growing in southeast Alaska. Can. J. For. Res. 51(11): 1707–1717.

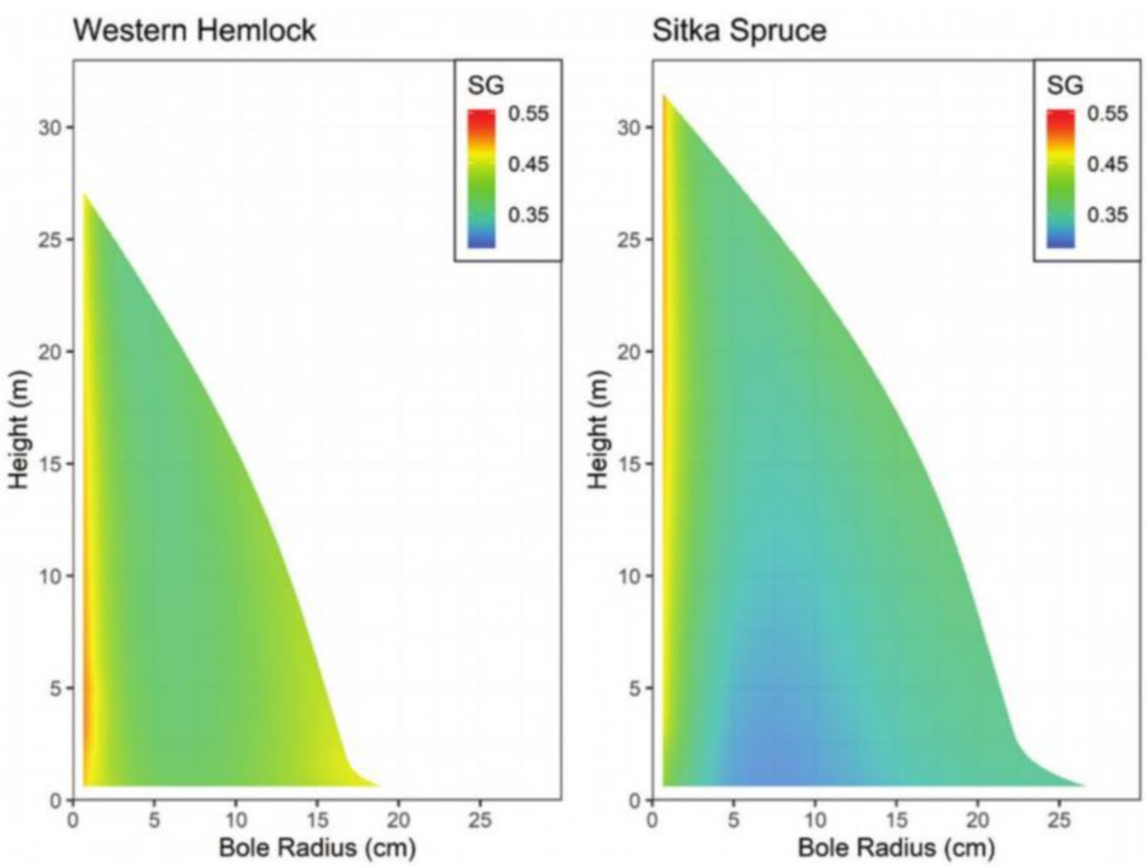

and also for spruce depicted by Volkert (1941) as shown in Kollmann and Côté (1968).

Observations and future research directions

The maps examined for North American conifers represent many approaches which provide a series of incremental improvements with time. Various methods have been used to measure wood properties producing maps of differing resolution with the highest having ring-level information, e.g., Evans et al. (2006). In terms of representation, data has been averaged (if multiple trees were assessed, but often only one tree was examined) and plotted with interpolation (Mora and Schimleck 2009) or models fitted to wood property data (Tian et al. 1995*a*,*b*, Moore et al. 2014 and 2015; Dahlen et al. 2018, 2021*a*,*b*, 2023) which were subsequently used to produce maps. Both absolute and relative radial positions and heights have been utilized, and radial positions have also been represented by distance and ring number.

Amongst the first published maps for North American conifers are those reported by Cooper (1960) and Risi and Zeller (1960). Both are low resolution as density was measured on samples representing multiple rings. The map reported by (Cooper 1960) is notable as it utilizes contour lines to identify different density regions. There are earlier examples of maps utilizing contour lines, e.g., Trendelenburg (1935), Volkert (1941) as shown in Kollmann and Côté (1968), and Turnbull (1947), but Cooper (1960) is likely the first map for a North American conifer species using this approach. More recent maps all utilize color gradients to represent similar wood property zones.

This is the first comprehensive review of wood property maps for North American conifers, and we attempted to use our examination of maps collectively to enhance our understanding of within-tree wood property variation. For plantation grown pines (Table 1) almost all maps can be categorized into two groups related to tracheid differentiation processes. The first includes properties that are directly associated with secondary cell wall formation, e.g., density, and the second group relates directly to tracheid enlargement, e.g., tracheid length and width, and the characteristics of the secondary cell wall. The second group includes MFA and stiffness. MFA is a result of secondary cell wall thickening indicating that the age at which this occurs, and the location (height) of the cambium within a stem, are important in addition to cell size. Of the various properties we examined, only tracheid radial diameter (Schimleck et al. 2020), perimeter (Evans et al. 1995, 1999) and spiral grain angle failed to have a map consistent with either group. Amongst the wood properties examined, spiral grain angle is unique as it is not related to either of the tracheid differentiation processes described.

Similar conclusions were not possible for maps based on trees from natural forests (Table 2). Density maps representing the same species grown on different sites were quite different (Jozsa and Kellogg 1986; Jozsa et al. 1998; Vaughan 2020) indicating site had a large effect on patterns of wood property variation within-trees. The remaining studies of trees from natural forests were frequently limited to a single tree and very few studies examined multiple properties.

Further the review revealed that wood property maps are extremely limited for most North American conifers, especially examples representing plantation grown species having Type 2 and 3 radial density variation. The only published maps for additional properties amongst these species are for stiffness (Todoroki et al. 2012) and coarseness (Defo et al. 2009) in Douglas-fir. A concentrated research program is required for the most commercially important of these species, and preliminary work should examine the within-tree variation of density of trees from planted forests, with later work considering additional properties.

An important observation is that three types of density maps, consistent with the three patterns of radial variation (Types 1, 2, and 3) as defined by Panshin and de Zeeuw (1980), are likely. The density maps listed in Table 1, with one exception (So et al. 2002), all had Type 1 radial density variation. Maps for western hemlock and Sitka spruce (Dahlen et al. 2021*b*) were clearly different and had Type 2 radial density variation. Similarly, a map for western red cedar (Type 3) was different to all other density maps reported (Wellwood and Jurazs 1968).

There is sufficient information regarding radial variation across species to suggest maps for properties such as MFA, and tracheid length in Type 2 and 3 conifers could be similar to maps reported for these properties in loblolly and radiata pine. Radially, MFA decreases with increasing distance from the pith with few exceptions (Barnett and Jeronimidis 2003; Lachenbruch et al. 2011). A radial decrease in MFA has been observed for balsam fir (*Abies balsamea* (L.) Mill.) (Giroud et al. 2021), black spruce (Alteyrac et al. 2006; Giroud et al. 2015; Giroud et al. 2021), Sitka spruce (Auty et al. 2018), white spruce (*Picea glauca* (Moench) Voss) (Giroud et al. 2021), and lodgepole pine (*Pinus contorta* Douglas) (Hayatgheibi et al. 2018). Similarly, Jozsa and Middleton (1994) state that "based on work done to date, it is likely that in all British Columbia softwoods fiber length is shortest next to the pith at all height positions in the stem, and it increases radially outward with age". These trends were also observed for tracheid length at various heights in Douglas-fir (Jozsa and Middleton 1994), white spruce (Mvolo et al. 2015*a*, *b*), and northern white cedar (*Thuja occidentalis* L.) (Bouslimi et al. 2014). Reported exceptions are English yew (*Taxus baccata* L.) (Keunecke et al. 2009) and Pacific yew (*Taxus brevifolia* Nutt.) (Fox and Schimleck 2024) where MFA shows little radial variation.

These observations suggest that across species, within-tree variability may be more consistent than individual studies suggest. Future research should aim to understand how generalizable tree maps are within and amongst species. For example, what effects do advanced genetics (Li et al. 1999) and silvicultural treatments, such as planting density, thinning, and fertilization have on property maps? Effects can be expected to vary by species. In loblolly pine it is unlikely that treatments will change the recognized Type 1 radial density pattern (Schimleck et al. 2022), whereas in western red cedar data reported by Fabris (2000) indicates that increased planting density can shift radial density variation from a Type 3 to a Type 2 pattern. Can we understand these effects well enough to predict how property maps should appear?

Further research should also examine if observations across commercially important North American conifers regarding the categorization of density maps as Type 1–3, and the predicted similarity of MFA and tracheid length maps can be extended to commercially important conifers in other parts of the world. An even broader question to consider is are the observations regarding map types applicable to hardwood species? Research in plantation-grown shining gum (*Eucalyptus nitens* (H.Deane & Maiden) Maiden) (Evans et al. 2000) indicates that MFA trends are similar to those observed in species such as loblolly and radiata pine.

A final consideration regarding future studies of within-tree variation is the utilization of existing and emerging technologies for wood property evaluation. A variety of nondestructive measurement options now exist (Schimleck et al. 2019) and they greatly enhance our ability to produce maps for multiple wood properties. Ideally, future property maps will be developed with methodologies that are consistent as it would allow direct comparison of property values and maps across studies. Developments in machine learning also holds promise as it will offer new options for modeling wood property variation but as with property measurements movement toward consistency in mapping approaches is important.

Acknowledgements

Support for the loblolly pine component of this work was provided by the Georgia TIP3 program and is gratefully acknowledged. The authors thank the UGA Wood Quality Consortium for collecting the loblolly pine samples and for sample preparation. Gratitude is also extended to Joshua Limbaugh (USDA Forest Service, Forest Products Laboratory) for drawings (Figs. 1 and 3) adapted from those in the literature.

Article information

History dates

Received: 28 May 2024
Accepted: 28 August 2024
Accepted manuscript online: 26 September 2024
Version of record online: 15 January 2025

Copyright

Data availability

Data generated or analyzed during this study are provided in full within the published article.

Author information

Author ORCIDs

Laurence Schimleck https://orcid.org/0000-0003-1958-6059
Thomas L. Eberhardt https://orcid.org/0000-0002-8818-4822

Author contributions

Conceptualization: LS, JD
Investigation: LS, JD, TLE, IO
Visualization: JD, CM, FA, TLE
Writing – original draft: LS, JD, CM, FA, TLE, IO
Writing – review & editing: LS, JD, CM, FA, TLE, IO

Competing interests

The authors declare no competing interests.

References

Albert, D.J., Clark, T.A., Dickson, R.L., and Walker, J.C.F. 2002. Using acoustics to sort radiata pine pulp logs according to fibre characteristics and paper properties. Int. For. Rev. **4**(1): 12–19.

Alteyrac, J., Cloutier, A., Ung, C.-H., and Zhang, S.Y. 2006. Mechanical properties in relation to selected wood characteristics of black spruce. Wood Fiber Sci. **38**(2): 229–237.

Auty, D., Moore, J.R., Achim, A., Lyon, A., Mochan, S., and Gardiner, B.A. 2018. Effects of early respacing on the density and microfibril angle of Sitka spruce wood. Forestry, **91**: 307–319. doi:10.1093/forestry/cpx004.

Barnett, J.R., and Jeronimidis, G. 2003. Wood quality and its biological basis. Blackwell Publishers, Oxford, UK.

Bouslimi, B., Koubaa, A., and Bergeron, Y. 2014. Anatomical properties in *Thuja occidentalis*: variation and relationship to biological processes. IAWA J. **35**(4): 363–384. doi:10.1163/22941932-00000072.

Burdon, R.D., Kibblewhite, R.P., Walker, J.C.F., Megraw, R.A., Evans, R., and Cown, D.J. 2004. Juvenile versus mature wood: a new concept, orthogonal to corewood versus outerwood, with special reference to *Pinus radiata* and *P. taeda*. For. Sci. **50**(4): 399–415.

Cooper, G.A. 1960. Specific gravity of red pine as related to stem- and crown-formed wood. Iowa State J. Sci. **34**(4): 337–349.

Cown, D.J. 1974. Wood density of radiata pine: its variations and manipulation. N. Z. J. For. **19**: 84–92.

Cown, D.J., and McConchie, D.L. 1980. Wood property variations in an old-crop stand of radiata pine. N. Z. J. For. Sci. **10**(3): 508–520.

Cown, D.J., McConchie, D.L., and Young, G.D. 1991. Radiata pine: wood properties survey. FRI Bulletin No. 50, Rotorua, New Zealand, 50p.

Dahlen, J., Auty, D., and Eberhardt, T.L. 2018. Models for predicting specific gravity and ring width for loblolly pine from intensively managed plantations, and implications for wood utilization. Forests, **9**(6): 292. doi:10.3390/f9060292.

Dahlen, J., Auty, D., and Lowell, E. 2021b. Modeling specific gravity and diameter inside bark of western hemlock and Sitka spruce growing in southeast Alaska. Can. J. For. Res. **51**(11): 1707–1717. doi:10.1139/cjfr-2020-0345.

Dahlen, J., Auty, D., Eberhardt, T.L., Schimleck, L.R., and Pokhrel, N.R. 2023. Models for predicting the within-tree variation of ultrasonic velocity and dynamic modulus of elasticity for plantation loblolly pine. Forestry, **96**(4): 588–604. doi:10.1093/forestry/cpac063.

Dahlen, J., Nabavi, M., Auty, D., Schimleck, L., and Eberhardt, T.L. 2021a. Models for predicting the within-tree and regional variation of tracheid length and width for plantation loblolly pine. Forestry, **94**: 127–140. doi:10.1093/forestry/cpaa018.

Defo, M., Goodison, A., and Uy, N. 2009. A method to map within-tree distribution of fibre properties using SilviScan-3 data. For. Chron. **85**(3): 409–414. doi:10.5558/tfc85409-3.

Downes, G.M., Drew, D., Battaglia, M., and Schulze, D. 2009. Measuring and modelling stem growth and wood formation: an overview. Dendrochronologia, **27**: 147–157. doi:10.1016/j.dendro.2009.06.006.

Downes, G.M., Meder, R., Ebdon, N., Bond, H., Evans, R., Joyce, K., and Southerton., S. 2010. Radial variation in cellulose content and Kraft pulp yield in *eucalyptus nitens* using near-infrared spectral analysis of air-dry wood surfaces. J. Near Infrared Spectrosc. **18**(2): 147–154. doi:10.1255/jnirs.875.

Eberhardt, T.L., and Samuelson, L.J. 2015. Collection of wood quality data by X-ray densitometry: a case study with three southern pines. Wood Sci. Technol. **49**: 739–753. doi:10.1007/s00226-015-0732-x.

Eberhardt, T.L., So, C.L., and Leduc, D.J. 2018. Wood variability in mature longleaf pine: differences related to cardinal direction for a softwood in a humid subtropical climate. Wood Fiber Sci. **50**(3): 323–336. doi:10.22382/wfs-2018-031.

Eberhardt, T.L., So, C.L., and Leduc, D.J. 2019. Wood property maps showing wood variability in mature longleaf pine: does getting old change juvenile tendencies? Wood Fiber Sci. **51**(2): 193–208. doi:10.22382/wfs-2019-020.

Evans, R. 1994. Rapid measurement of the transverse dimensions of tracheids in radial wood sections from *Pinus radiata*. Holzforschung, **48**: 168–172. doi:10.1515/hfsg.1994.48.2.168.

Evans, R. 1999. A variance approach to the X-ray diffractometric estimation of microfibril angle in wood. Appita J. **52**(4): 283–289, 294.

Evans, R. 2006. Wood stiffness by X-ray diffractometry, *In* Characterization of the cellulosic cell wall. *Edited by* D.D. Stokke and L.H.C. Groom. Blackwell Publishing, Ames, IA. pp. 138–146.

Evans, R., Downes, G., Menz, D., and Stringer, S. 1995. Rapid measurement of variation in tracheid transverse dimensions in a radiata pine tree. Appita J. **48**(2): 134–138.

Evans, R., Ilic, J., Fife, D., Gritton, D., Mattay, J., and Morrow, A. 2006. Comprehensive distribution of wood quality characteristics in pine butt logs. WQI Ltd. Report No. Str 23, 22p.

Evans, R., Kibblewhite, R.P., and Lausberg, M. 1999. Relationships between wood and pulp properties of twenty-five 13 year old radiata pine trees. Appita J. **52**(2): 132–139.

Evans, R., Kibblewhite, R.P., and Riddell, M.J.C. 2004. Contribution of wood density, microfibril angle and wood stiffness to the properties of handsheets from eleven radiata pine clones. Proc. 58th Appita Gen. Conf., Canberra, Australia.

Evans, R., Stringer, S., and Kibblewhite, R.P. 2000. Variation of microfibril angle, density and fibre orientation in twenty-nine *eucalyptus nitens* trees. Appita J. **53**(6): 450–457.

Fabris, S. 2000. Influence of cambial ageing, initial spacing, stem taper and growth rate on the wood quality of three coastal conifers. PhD Thesis. The University of British Columbia, Vancouver, Canada, 250p.

Fernow, B.E. 1896. Southern pine-mechanical and physical properties. U.S. Department of Agriculture, Division of Forestry, Circular No. 12. 12pp.

Fox, G.O., and Schimleck, L.R. 2024. Microstructural properties of Pacific yew as determined with SilviScan. IAWA J. (submitted).

Giroud, G., Defo, M., and Bégin, J. 2021. Determination of radial profiles of wood properties using a near infrared scanning system. J. Near Infrared Spectrosc. **29**(1): 24–32. doi:10.1177/0967033520967324.

Giroud, G., Defo, M., Bégin, J., and Ung, C.-H. 2015. Application of near-infrared spectroscopy to determine the juvenile–mature wood transition in black spruce. For. Prod. J. **65**(3/4): 129–138.

Groom, L., Mott, L., and Shaler, S. 2002. Mechanical properties of individual southern pine fibers. Part III. Global relationships between fiber properties and fiber location within an individual tree. Wood Fiber Sci. **34**(2): 238–250.

Hardin, J.W., Leopold, D.J., and White, F.M. 2001. Harlow and Harrar's textbook of dendrology 9th ed. McGraw-Hill, NY, 534 p.

Harris, J.M. 1969. The use of beta rays in determing wood properties—Part 3. Summarizing radial variations in wood density. N. Z. J. Sci. **12**: 419–431.

Hayatgheibi, H., Forsberg, N.E.G., Lundqvist, S.-O., Mörling, T., Mellerowicz, E.J., Karlsson, B., et al. 2018. Genetic control of transition from juvenile to mature woodwith respect to microfibril angle in Norway spruce (*Picea abies*) and lodgepole pine (*Pinus contorta*). Can. J. For. Res. **48**: 1358–1365. doi:10.1139/cjfr-2018-0140.

Jordan, L., He, R.C., Hall, D.B., Clark, A., and Daniels, R.F. 2007. Variation in loblolly pine ring microfibril angle in the Southeastern United States. Wood Fiber Sci. **39**(2): 352–363.

Jozsa, L.A., and Kellogg, R.M. 1986. An exploratory study of the density and annual ring weight trends in fast-growth coniferous woods in British Columbia. Forintek Canada Corp. Tech. Rep., 43 p.

Jozsa, L.A., and Middleton, G.R. 1994. A discussion of wood quality attributes and their practical implications. Forintek Canada Corp. SP34, 42 p.

Jozsa, L.A., Munro, B.D., and Gordan, J.R. 1998. Basic wood proeprties of second-growth western hemlock. Forintek Canada Corp. SP38, 51 p.

Keunecke, D., Evans, R., and Niemz, P. 2009. Microstructural properties of common yew and Norway spruce determined with SilviScan. IAWA J. **30**(2): 165–178. doi:10.1163/22941932-90000212.

Kibblewhite, R.P., Evans, R., and Riddell, M.J.C. 2003. Kraft handsheet, and wood tracheid and chemical property interrelationships for 50 individual radiata pine trees. Appita J. **56**(3): 229–233.

Kollmann, F.F.P., and Côté, W.A. 1968. Principles of Wood Science. I Solid Wood. Springer-Verlag, New York, p 172.

Lachenbruch, B., Moore, J.R., and Evans, R. 2011. Radial variation in wood structure and function in woody plants, and hypotheses for its occurrence. In Size- and Age-Related Changes in Tree Structure and Function. *Edited by* F.C. Meinzer, B. Lachenbruch and T.E. Dawson. Springer-Verlag, Berlin, Germany, pp 121–164.

Leitch, M., and Miller, S. 2017. Optimizing wood utilization based on whole tree inherent property maps. In Wood is Good. Current Trends and Future Prospects in Wood Utilization. *Edited by* K.K. Pandey, V. Ramakantha, S.S. Chauhan and A.N.A. Kumar. Springer Nature, Singapore, pp 3–17.

Li, B., McKeand, S., and Weir, R. 1999. Tree improvement and sustainable forestry—impact of two cycles of loblolly pine breeding in the U.S.A. For. Genet. **6**(4): 229–234.

Li, X.G., Evans, R., Gapare, W., Yang, X., and Wu, H.X. 2014. Characterizing compression wood formed in radiata pine branches. IAWA J. **35**: 385–394. doi:10.1163/22941932-00000073.

Longuetaud, F., Mothe, F., Fournier, M., Dlouha, J., Santenoise, P., and Deleuze, C. 2016. Within-stem maps of wood density and water content for characterization of species: a case study on three hardwood and two softwood species. Ann. For. Sci. **73**(3): 601–614. doi:10.1007/s13595-016-0555-4.

Lundqvist, S.-O., Ekenstedt, F., Hedenberg, O., and Twaddle, A. 2005. Wood and fiber properties of loblolly pine in the southeast USA. Variations and prediction models. Fifth workshop, Connection Between Forest Resources and Wood Quality: Modelling Approaches and Simulation Software. Waiheke Island Resort, New Zealand.

Luxford, R.F., and Markwardt, L.J. 1932. The strength and related properties of redwood. Tech. Bull. 305. U.S. Dep. Agric., Washington D.C., 48 p.

Moore, J.R., Cown, D.J., and McKinley, R.B. 2014. Modelling microfibril angle variation in New Zealand-grown radiata pine. N. Z. J. For. Sci. **44**: 25. doi:10.1186/s40490-014-0025-4.

Moore, J.R., Cown, D.J., and McKinley, R.B. 2015. Modelling spiral grain angle variation in New Zealand-grown radiata pine. N. Z. J. For. Sci. **45**: 9. doi:10.1186/s40490-015-0046-7.

Mora, C.R., and Schimleck, L.R. 2009. Determination of within-tree variation of *Pinus taeda* wood properties by near infrared spectroscopy. Part 2: whole-tree wood property maps. Appita J. **62**(3): 232–238.

Mott, L., Groom, L., and Shaler, S. 2002. Mechanical properties of individual southern pine fibers. Part II. Comparison of earlywood and latewood fibers with respect to tree height and juvenility. Wood Fiber Sci. **34**(2): 221–237.

Mvolo, C.S., Koubaa, A., Beaulieu, J., Cloutier, A., and Mazerolle, M.J. 2015a. Variation in wood quality in white spruce (*Picea glauca* (Moench) Voss). Part I. Defining the juvenile–mature wood transition based on tracheid length. Forests **6**: 183–202. doi:10.3390/f6010183.

Mvolo, C.S., Koubaa, A., Defo, M., Beaulieu, J., Yemele, M.C., and Cloutier, A. 2015b. Prediction of tracheid length and diameter in white spruce (*Picea glauca*). IAWA J. **36**(2): 186–207. doi:10.1163/22941932-00000095.

Nabavi, M., Dahlen, J., Schimleck, L., Eberhardt, T.L., and Montes, C. 2018. Regional calibration models for predicting loblolly pine tracheid properties using near-infrared spectroscopy. Wood Sci. Technol. **52**: 445–463. doi:10.1007/s00226-018-0986-1.

Okkonen, E.A., Wahlgren, H.E., and Maeglin, R.R. 1972. Relationships of specific gravity to tree height in commercially important species. For. Prod. J. **22**(7): 37–41.

Panshin, A.J., and de Zeeuw, C. 1980. Textbook of wood technology, 4th edn. McGraw-Hill, New York.

Paul, B.H. 1963. The application of silviculture in controlling the specific gravity of wood. Tech. Bull. 1288. U.S. Dep. Agric. For. Serv., Madison, WI, 97 p.

Phillips, E.W.J. 1960. The beta-ray method of determining the density of wood and the proportion of summer wood. J. Inst. Wood Sci. **5**: 16–27.

Phillips, E.W.J., Adam, E.H., and Hearmon, R.F.S. 1962. The measurement of density variation within the growth rings in thin sections of wood using beta particles. J. Inst. Wood Sci. **10**: 11–28.

Polge, H. 1964. Le bois juvénile les conifers. Rev. Forest. Franc. **16**: 474–505.

Raymond, C.A., Thomas, D.S., and Henson, M. 2010. Predicting pulp yield and pulp productivity of *eucalyptus dunnii* using acoustic techniques. Aust. For. **73**(2): 91–97. doi:10.1080/00049158.2010.10676314.

Risi, J., and Zeller, E. 1960. Specific gravity of the wood of black spruce (*Picea mariana* (Mill.) B.S.P.) grown on a Hylocomium-Cornus site type. Laval Univ. For. Res. Found. Quebec, Canada Contr. 6, 70 pp.

Schimleck, L., Antony, F., Mora, C., and Dahlen, J. 2018. Comparison of whole-tree wood property maps for 13- and 22-year-old loblolly pine. Forests **9**: 287. doi:10.3390/f9060287.

Schimleck, L., Antony, F., Mora, C., and Dahlen, J. 2020. Whole-tree tracheid property maps for loblolly pine at different ages. Wood Sci. Technol. **54**(3): 683–701. doi:10.1007/s00226-020-01180-7.

Schimleck, L., Antony, F., Mora, C., and Dahlen, J. 2021a. Mapping variation of handsheet properties within loblolly pine trees. Nord Pulp Pap. Res. J. **36**(3): 387–398. doi:10.1515/npprj-2020-0109.

Schimleck, L., Antony, F., Mora, C., and Dahlen, J. 2021b. Whole-tree maps of pulp yield and lignin content for loblolly pine. SN Applied Sciences **3**: 468. doi:10.1007/s42452-021-04443-5.

Schimleck, L., Dahlen, J., Apiolaza, L., Downes, G., Emms, G., Evans, R., et al. 2019. Non-destructive evaluation techniques and what they tell us about wood property variation. Forests **10**: 728. doi:10.3390/f10090728.

Schimleck, L.R., and Evans, R. 2004. Estimation of *P. radiata* D. Don tracheid morphological characteristics by near infrared spectroscopy. Holzforschung **58**(1): 66–73. doi:10.1515/HF.2004.009.

Schimleck, L.R., and Tsuchikawa, S. 2021. *Application of NIR spectroscopy to wood and wood derived products* (Chapter 37). In: “The Handbook of Near-Infrared Analysis” Fourth Edition. CRC Press, Boca Raton, Florida, 759–780.

Schimleck, L.R., Dahlen, J., and Auty, D. 2022. Radial patterns of specific gravity variation in North American conifers. Can. J. For. Res. **52**(6): 889–900. doi:10.1139/cjfr-2021-0338.

So, C.-L., Groom, L.H., Rials, T.G., Snell, R., Kelley, S.S., and Meglen, R. 2002. Rapid assessment of the fundamental property variation of wood. Proc. 11th Biennial Southern Silvicultural Research Conference, K.W. Outcalt(Ed.). 20-22 March 2001, Knoxville, TN. Gen. Tech. Rep. SRS-48 USDA Forest Service, Southern Research Station, Asheville, NC, pp 176–180.

Thumm, A., Riddell, M., Nanayakkara, B., Harrington, J., and Meder, R. 2016. Mapping within-stem variation of chemical composition by near infrared hyperspectral imaging, J. Near Infrared Spectrosc. **24**(6): 605–616. doi:10.1255/jnirs.1206.

Tian, X., Cown, D.J., and Lausberg, M.J.F. 1995*a*. Modelling of *Pinus radiata* wood properties. Part 2: basic density. N. Z. J. For. Sci. **25**(2): 214–230.

Tian, X., Cown, D.J., and Lausberg, M.J.F. 1995*b*. Modelling of *Pinus radiata* wood properties. Part 1: spiral grain. N. Z. J. For. Sci. **25**(2): 200–213.

Todoroki, C.L., Lowell, E.C., Dykstra, D.P., and Briggs, D.G. 2012. Maps and models of density and stiffness within individual Douglas-fir trees. N. Z. J. For. Sci. **42**: 1–13.

Trendelenburg, R. 1935. Schwankungen des raumgewichts wichtiger nadelhäolzer nach wuchsgebiet, standort und einzelstamm. Z. Ver. Dtsch. Ing. **79**(4): 85–89 (in German).

Turnbull, J.M. 1947. Some factors affecting density in pine stems. South. Afr. For. J. **16**(1): 22–43.

Uprichard, J.M., and Lloyd, J.A. 1980. Influence of tree age on the chemical composition of radiata pine. Holzforschung N. Z. J. For. Sci. **10**(3): 551–557.

Vaughan, D. 2020. Wood properties of southwestern Pinus ponderosa and relationships with silviculture, climate, and wood products. PhD Thesis. Northern Arizona, Flagstaff, AZ, 108p.

Vaughan, D., Auty, D., Kolb, T., Dahlen, J., Meador, A.J.S., and Mackes, K.H. 2021. Wood density variation in naturally regenerated stands of Pinus ponderosa in northern Arizona, USA. Can. J. For. Res. **51**(4): 583–594. doi:10.1139/cjfr-2020-0245.

Via, B.K., Shupe, T.F., Stine, M., So, C.-L., and Groom, L.H. 2005. Tracheid length prediction in *Pinus palustris* by means of near infrared spectroscopy: the influence of age. Holz Roh. Werkst. **63**(3): 231–236. doi:10.1007/s00107-004-0567-x.

Volkert, E. 1941. Investigations regarding the level and variation of wood density in softwood. Schriften Hermann Göring Akad Dtsch Forstwissenschaft **2**: 1–133 (in German).

Wellwood, R.W., and Jurazs, P.E. 1968. Variation in sapwood thickness, specific gravity and tracheid length in western red cedar. For. Prod. J. **18**(12): 37–46.

Zhang, D., and Stanturf, J. 2008. Forest plantations. In: Ecosystems. Vol. 2 of Encyclopedia of Ecology. *Edited by* S.E. Jørgensen and B.D. Fath, Elsevier, Oxford. pp. 1673–1680.